J|A|C|S ARTICLES

Published on Web 09/18/2009

Size-Scaling of Proton Conductivity in Amorphous Aluminosilicate Acid Thin Films

Yoshitaka Aoki,*,† Hiroki Habazaki,† and Toyoki Kunitake‡

Graduate School of Engineering, Hokkaido University, N13W8, Kita-ku, Sapporo, 060-8628, Japan, NanoMembrane Technologies Inc., Wako-RIKEN IP 406, 2-3-13 minami, Wako, 351-0104, Japan

Received June 7, 2009; E-mail: y-aoki@eng.hokudai.ac.jp

Abstract: Amorphous aluminosilicate nanofilms, *a*-$Al_{0.1}Si_{0.9}O_x$, exhibit unique size-enhancement of the proton conductivity along the thickness direction because of the presence of the zeolite-like, acid site network with the mesoscopically sized dimension inside glass matrix. The dense films with the thickness of 22−1400 nm were uniformly formed over the electrode substrate in nanometer thickness precision by multiple spin-coating with a mixed precursor sol. XANES measurements indicated that the basic framework of *a*-$Al_{0.1}Si_{0.9}O_x$ films was similar to the zeolitic one, consisting of the corner-linkage of SiO_4 and AlO_4 tetrahedral units. These films revealed the complex temperature- and humidity-dependency of proton conductivity by the existence of two kinds of protonic carriers: Brønsted acidic protons and Lewis acidic protons. The Brønsted acidic protons could be persistent in amorphous films at around 500 °C, as checked by thermal desorption spectroscopy, so that the film exhibited the humidity-independent proton conductivity at temperatures above 300 °C. Furthermore, the conductivity across the film σ increased in a power low by reduction of the film thickness d to less than 120 nm as $\sigma \propto d^{-\tau}$, and it was saturated when the thickness become less than 40 nm. The observed scaling index τ was 2.2 in agreement with the value of the theoretical index (2.3) of cluster size scaling in a three-dimensional percolation system. This conduction behavior is explicable by finite size-scaling of the highly conductive pathway based on the interconnected Brønsted acid centers in the range of a few tens to hundreds of nanometers.

Introduction

Fuel cells are attractive alternatives to combustion engines for electrical power generation because of their high efficiency and low pollution levels. The cells operating at intermediate temperatures between 150 and 400 °C (IT-FC) are of particular interest, because this temperature range allows the use of less precious metal catalysts and alcohol fuel, enables in situ reforming of hydrocarbon fuels, and facilitates simpler module assembly.[1,2] Unfortunately, these advantages are not available if electrolyte membranes of the conventional organic polymer are used, because the protonic transport relies on the diffusion of H_3O^+ ions (vehicular mechanism),[3] which limits the operating temperature below the dehydration temperature of ca. 100 °C. Anhydrous proton conductors can alleviate this problem, because the conductivity arises from the migration of the native protons via jumps between adjacent oxide ions by a series of making and breaking of hydrogen bonds (Grotthuss mechanism).[3] Solid acids are adopt to this group and the simple inorganic oxo-acid salts, such as CsH_2PO_4 and $CsHSO_4$, have been examined.[4−9] These salts provide the practical conductivity of 1×10^{-2} Ω^{-1} cm^{-1} above the super protonic transition temperature at around 230 °C. However, they have limitation on a practical use because of the hygroscopicity and the ductility above the transition temperature.[4,6−8] Therefore, the design of inorganic anhydrous proton conducting membranes that are stable and provide good performance at intermediate temperatures raises major challenge. This study presents the new type of anhydrous proton conductor harnessing the abundant Brønsted acid centers on robust silicate framework.

Zeolites are a class of crystalline aluminosilicates that are built up by corner-linkage of SiO_4 and AlO_4 tetrahedra forming a three-dimensional network. The isomorphous substitution of Si^{4+} by Al^{3+} causes a negative excess charge of the framework made of 4-fold-connected MO_4 tetrahedra. Therefore, zeolites accommodate a large amount of protons by the anionic framework and often exhibit strong Brønsted acidity even at elevated temperatures in various catalysis processes.[10] These properties intend that zeolitic compounds are attractive as a thermally stable, anhydrous proton conductor. In fact, certain

† Hokkaido University.
‡ NanoMembrane Technologies Inc.

(1) Steele, B. C. H.; Heinzel, A. *Nature* **2001**, *414*, 345.
(2) Hibino, T.; Hashimoto, A.; Inoue, T.; Tokuno, J.; Yoshida, S.; Sano, M. *Science* **2000**, *288*, 2031.
(3) Kreuer, K.-D. *Chem. Mater.* **1996**, *8*, 641.
(4) Haile, S. M.; Chisholm, C. R. I.; Sasaki, K.; Boysen, T. A.; Uda, T. *Faraday Discuss.* **2007**, *134*, 17.
(5) Boysen, D. A.; Uda, T.; Chisholm, C. R. I.; Haile, S. M. *Science* **2004**, *303*, 68.
(6) Boysen, D. A.; Haile, S. M.; Liu, H. J.; Secco, R. A. *Chem. Mater.* **2003**, *15*, 727.
(7) Ponomareva, V. G.; Lavrova, G. L. *Solid State Ionics* **2001**, *145*, 197.
(8) Boysen, D. A.; Chisholm, C. R. I.; Haile, S. M.; Narayanan, S. R. *J. Electrochem. Soc.* **2000**, *147*, 3610.
(9) Haile, S. M.; Boysen, D. A.; Chisholm, C. R. I.; Merle, R. B. *Nature* **2001**, *410*, 910.
(10) (a) Corma, A.; Garcia, H. *Chem. Rev.* **2003**, *103*, 4307. (b) Farneth, W. E.; Gorte, R. J. *Chem. Rev.* **1995**, *95*, 615.

zeolitic compounds give proton conductivity of 1×10^{-6} S cm^{-1} even in a dry atmosphere.[11−14] In spite of the potential proton conductivity, the conventional zeolitic compound is not considered as a practical candidate of the electrolyte membrane in fuel cells and other electrochemical devices, because polycrystalline zeolites, even if proton conducting, will not effectively suppress permeation of fuel gases (typically hydrogen and oxygen molecules) because of their characteristic cage structures and voids at grain boundaries.

A noncrystalline aluminosilicate film retaining the zeolitic anionic framework, if available, is very promising by the following reasons: (1) amorphous oxide tend to be nongranular, dense layer due to the three-dimensional network of covalent M−O bonding, and (2) reducing electrolyte thickness into nanometer region significantly reduce the ohmic loss at a given operating temperature.[1,15−19] Previously, we reported that amorphous aluminosilicate thin films, *a*-$Al_nSi_{1-n}O_x$, prepared by sol−gel spin-casting exhibit the practical proton conductivity along the thickness direction in a dry atmosphere in the intermediate temperature range, even though the corresponding bulk powder sample shows rather poor conductivity.[20,21] In addition, the conductivity was increased in a power-law by reduction of thickness into the sub-100 nm regime.[22] It is important to clarify the origin of these unique conduction behaviors, because the area-specific resistance of films, which is a practical measure of the efficiency of electrolyte membrane, is lower than the ideal value (0.2 Ω cm^2)[23] at temperatures below 400 °C in dry air. Herein, we demonstrated that the elevated proton conductivity of *a*-$Al_nSi_{1-n}O_x$ film arises from the highly conductive acid site networks, which extend in the range of a few tens of nanometers to hundreds of nanometers inside the glass matrix. If the thickness is within this size range, the highly conductive network percolates from one side of film to the opposite and the conductivity of film increases. The current results could be extended to more general way to design the ionic transport properties of various solid electrolyte materials.

Experimental Section

Amorphous aluminosilicate thin films, *a*-$Al_nSi_{1-n}O_x$, were prepared from mixed precursor solutions of tetraethoxysilane (TEOS) (Kanto Chemical) and aluminum *sec*-butoxide ($Al(O^sBu)_3$) (Kanto Chemical) with the Al/Si atomic ratio of 5/95, as reported in elsewhere.[20,21] The films were deposited on an electrode substrate in the layer-by-layer fashion by multiple spin-coating and hydrolysis. The precursor sol was prepared as follows. Appropriate doses of TEOS were added to 15 mL of 1-PrOH, and then H_2O (0.1 M hydrochloric acid) was added to the solution until the H_2O/Si molar ratio became 2/1. After stirring for 1 h at room temperature, $Al(O^sBu)_3$ was added to the stirred solution to the atomic ratio of Al/Si = 5/95, and the mixtures were further stirred at 70 °C for 30 min. The solution was diluted with 1-PrOH and the final concentration of the total metal atoms (Al + Si) in the precursor solution was adjusted in 40 mM for the films of <100 nm thickness and 100 mM for the films of ≥100 nm thickness. In this study, films with thicknesses of 22, 28, 40, 50, 60, 100, 120, 160, 300, and 1400 nm were prepared.

The precursor sols were spin-coated onto the ITO substrate at 3000 rpm for 40 s by a Mikasa 1H-D7 spin coater. The deposited gel layer was hydrolyzed by blowing hot air for 30 s (Iuchi hot gun), and the substrate was cooled to room temperature by blowing cold air for 20 s. These cycles of spin-coating, hydrolysis and cooling were repeated 10−40 times and the gel films thus obtained were annealed at 400 °C for 15 min. The combination of deposition and annealing was repeated more than 3 times, and the final annealing was performed at 450 °C for 1 h. ITO-coated glass slide (ITO layer: 40 nm thick) was used as an electrode substrate. ITO substrate was purchased from Aldrich and the surface was cleaned by sonicating in ethanol for 3 min before film deposition.

The morphology of $Al_nSi_{1-n}O_x$ films was characterized by scanning electron microscopy (SEM) (JEOL JSM-6500F). The specimen for SEM observation was coated with Pt. The cross-section transmission electron microscopy (TEM) was performed by Hitachi HD-2000 at an acceleration voltage of 200 kV. Specimens for the TEM observation were prepared on an Nb-sputtered Al plate (99.99%, 10 × 10 × 0.5 mm) by the procedure as mentioned above, and the ultrathin cross-sectional specimen was prepared by using a microtome (Leica, S55). X-ray photoelectron spectroscopy (XPS) was carried out with JEOL JPC-9010MC to measure the Al/Si atomic ratio of the film. Before XPS measurement, the surface of sample was sputtered by Ar^+ ion so as to form a clean surface and probe the inner of films. Temperature desorption spectroscopy (TDS) was performed for 10 × 10 mm^2 size specimens using an ultrahigh vacuum chamber system (ESCO TDS1400) equipped with a quadruple mass analyzer and infrared lamp heater. The spectra were recorded during heating from 50 to 700 at 30 °C min^{-1} under the initial pressure of 2.0×10^{-7} Torr. For the measurement, the film deposited on the Si wafer was used as a specimen. Prior to the measurement, the samples were exposed to D_2O-saturated air at 200 °C for 12 h. Al K-edge X-ray absorption near-edge spectroscopy (XANES) was carried out at B1A line in UVSOR at Institute of Molecular Science.

Ionic conductivity of $Al_nSi_{1-n}O_x$ films was measured by AC impedance method. Pt electrodes (100 nm thick, 1 mmϕ) were deposited on the top of the metal oxide films by ion etcher (Hitachi E1030) through a shadow mask to form a Pt/$Al_nSi_{1-n}O_x$/ITO stack. The electrical lead of Au fine wire (0.05 mmϕ) was attached to the top and bottom electrodes by using Au paste (Nilaco). Impedance spectroscopy measurement was carried out for the stack by the frequency response analyzer (Solartron 1260) in a frequency range of 10 to 1×10^7 Hz at AC amplitude of 20 mV. The specimens were first heated to 400 °C and kept at this temperature for 12 h under the controlled atmosphere, and then cooled to given temperatures of impedance measurement. All the measurements were carried out under dry and wet atmospheres after an hour of thermal equilibration at each temperature. The nonhumidified, "dry" air atmosphere was controlled by flowing a mixed gas of ultrapure O_2 and Ar (99.9999%) at a molar ratio of O_2/Ar = 1/4 through H_2O remover column at a rate of 100 mL min^{-1}. The humidified, "wet" air was prepared by bubbling the mixed gas at a rate of 100 cm^3 min^{-1} through pure H_2O at 25 °C (p_{H_2O} = 0.02 atm). Deuterated wet air was prepared by bubbling the mixed gas at a rate of 100 cm^3 min^{-1} through pure D_2O at 25 °C (p_{D_2O} = 0.02 atm). The wet hydrogen atmosphere was prepared by bubbling a mixed gas of

(11) Kreuer, K.-D.; Weppner, W.; Rabenau, A. *Mater. Res. Bull.* **1982**, *17*, 501.
(12) Hibino, T.; Akimoto, T.; Iwahara, H. *Solid State Ionics* **1993**, *67*, 71–76.
(13) Kundsen, N.; Anderson, E. K.; Anderson, I. G. K.; Norby, P.; Skou, E. *Solid State Ionics* **1993**, *61*, 153.
(14) Kwan, S. M.; Yeung, K. L. *Chem. Commun.* **2008**, 3631.
(15) Su, P.-C.; Chao, C.-C.; Shim, J. H.; Fasching, R.; Prinz, F. B. *Nano Lett.* **2008**, *8*, 2289.
(16) Shim, J. H.; Chao, C.-C.; Huang, H.; Prinz, F. B. *Chem. Mater.* **2007**, *19*, 3850.
(17) Yan, J.; Matsumoto, H.; Enoki, M.; Ishihara, T. *Electrochem. Solid-State Lett.* **2005**, *8*, A389.
(18) Ito, N.; Iijima, M.; Kimura, K.; Iguchi, S. *J. Power Sources* **2005**, *152*, 200.
(19) Ito, N.; Aoyama, S.; Masui, T.; Matsumoto, S.; Matsumoto, H.; Ishihara, T. *J. Power Sources* **2008**, *185*, 922.
(20) Aoki, Y.; Muto, E.; Nakao, A.; Kunitake, T. *Adv. Mater.* **2008**, *20*, 4387.
(21) Aoki, Y.; Muto, E.; Onoue, S.; Nakao, A.; Kunitake, T. *Chem. Commun.* **2007**, 2396.
(22) Aoki, Y.; Habazaki, H.; Kunitake, T. *Electrochem. Solid-State Lett.* **2008**, *11*, P13.
(23) Steele, B. C. H. *Curr. Opin. Solid State Mater. Sci.* **1996**, *1*, 684.

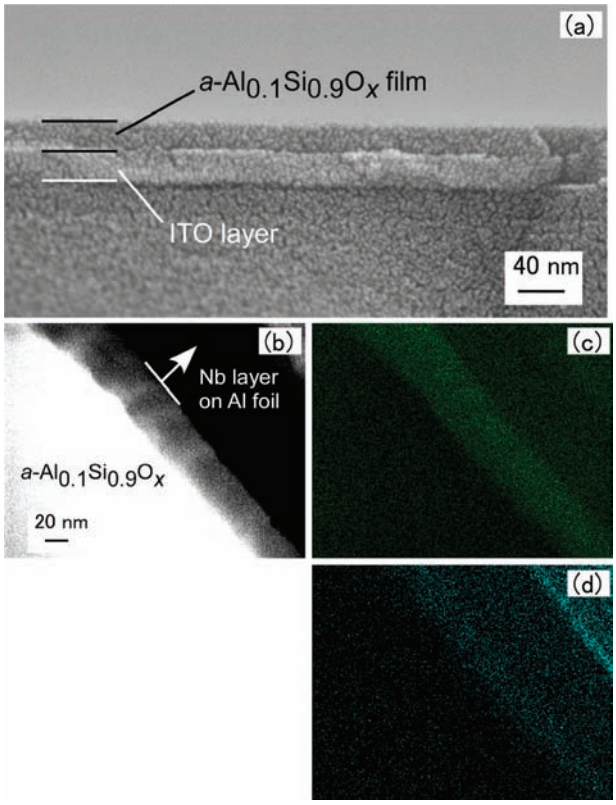

Figure 1. (a) Cross-section SEM images of a 28 nm thick $Al_{0.1}Si_{0.9}O_x$ film. (b−d) STEM-EDX images of the cross-section of a 60 nm thick $Al_{0.1}Si_{0.9}O_x$ film. (b) Electron micrograph, and EDX mapping images of (c) Al and (d) Si.

ultrapure H_2 and Ar at a molar ratio of H_2/Ar = 1/9 at a rate of 100 cm^3 min^{-1} through H_2O.

Results

The *a*-$Al_nSi_{1-n}O_x$ thin films prepared here were a single amorphous phase, as shown in the previous report.[20,21] All the films uniformly grow over a wide area in thickness precision of nm without pinholes, cracks and aggregates of particles (Figure 1). The film surface was very smooth as is the case with the glassy film. The thickness increment of these films in a single coating cycle turned out to be about 2 nm for 40 mM solution and 5 nm for 100 mM solution. The Al/Si ratio in films was 10/90 with a deviation of ±2 at all the thickness range, as checked by XPS measurement.[22] Figure 1b−d shows the scanning transmission electron microscopy and energy dispersive X-ray spectroscopy of *a*-$Al_nSi_{1-n}O_x$ films prepared on the Nb-sputtered Al plate. The film is made of a homogeneously mixed glass layer of alumina and silica. The metal-composition profiles across the film are very uniform with the Al/Si atomic ratio of 10/90. The Al/Si ratio is invariably greater than those of the corresponding precursor sol (Al/Si = 5/95), because the unreacted fraction of TEOS (bp ca. 170 °C) may be removed from the ultrathin deposited layer by evaporation during the hot air blow process after spin coating.

Clearly, the *a*-$Al_{0.1}Si_{0.9}O_x$ films exhibit impedance spectra characteristic of ion conducting film, that is, a small semicircle in the high-frequency region and a spike in the low-frequency region in Cole−Cole plots.[21,22,24] The obtained impedance spectra were analyzed by the nonlinear least-squares fitting so as to determine the proton conductivity (σ).[20,21,24]

The proton conductivity of the films with various thicknesses was measured in dry and wet atmospheres (Figure 2). The temperature dependence of σ in dry air is varied by thickness d. In case of d > 100 nm, the conductivity linearly increases with an activation energy E_a of 0.5 eV below 200 °C with a break at around 200 °C, and tends to increase with an increased E_a of 0.7−0.8 eV above 220 °C. With the films of d < 100 nm, the plot of σ in dry air is almost linear with an E_a of about 0.7 eV in the measured temperature range. Apparently, the value of σ in dry air drastically changes with thickness (Figure 3). Although σ of films is constant in the thickness of more than 160 nm, it increases with decreasing thickness in the region of less than 120 nm. Furthermore, σ becomes again constant at the thickness of less than 40 nm. The details are discussed latter.

There is almost no difference in σ of sub-100 nm-thick films in dry and wet atmospheres (Figure 2). In contrast, σ of the films with more than 120 nm thickness is clearly enhanced by humidity in the temperature region below 270 °C, but it remains unchanged by humidity above 300 °C. The E_a value of conductivity in wet air, which is determined from the slope, is 0.2−0.4 eV at T < 250 °C and 0.8 eV at T > 300 °C. σ of the 100 nm-thick film is slightly increased by humidity at $T \leq$ 150 °C, but the magnitude of the increment is relatively small compared to those of the thicker films. Apparently, the relatively high proton conductivity at elevated temperatures ($T \geq$ 300 °C) is not affected by the adsorbed water, if any, at all the thicknesses. For the films with 50 and 300 nm thickness, proton conductivity was also measured in a wet H_2 atmosphere (H_2/Ar = 1/9), indicating that σ in wet H_2 atmosphere is very similar to that in wet air in both films. Therefore, it is obvious that the protonic carriers in $Al_{0.1}Si_{0.9}O_x$ films are not given by the reaction of 1/2 $H_2 \leftrightarrows H_i^{\cdot} + e'$.

Proton conductivity in D_2O/air was also measured for the films with 50, 120, and 300 nm thickness (Figure 2). All the films show the clear H/D effect[3] on proton conductivity in the measured temperature ranges and σ in D_2O/air (σ_D) is lower than that in H_2O/air (σ_H) by a factor of σ_H/σ_D = 1.2−1.8. The temperature dependency of σ_D is very similar to σ_H in every thickness. Thus, it is concluded that ionic conductivity of our films is due to the hopping transport of proton.

The conductivity at temperatures above 400 °C was measured with a 300 nm thick film in dry air. The film sample was first heated to 400 °C and kept for 2 h and then cooled to given temperatures of impedance measurement, and was then heated to the subsequent temperature of measurement until 500 °C. The σ value in the first cooling process was reproduced in the second heating procedure at temperatures below 400 °C,[21] indicating that $Al_{0.1}Si_{0.9}O_x$ films does not show the irreversible changes of structure and composition below 400 °C. In the second heating procedure, σ monotonically increases until 450 °C, but the film exhibits an electrical breakdown at around 470 °C by showing large leakage current. Therefore, the conductivity measurement cannot be carried out above this temperature. These results indicate that $Al_{0.1}Si_{0.9}O_x$ films reveal the irreversible, structural deformation at around 500 °C.

Thermal desorption spectroscopy (TDS) was performed for *a*-$Al_{0.1}Si_{0.9}O_x$ films (50, 120, and 300 nm-thickness) and SiO_x films (300 nm-thickness) which were treated at 200 °C for 12 h in D_2O/air atmosphere prior to measurement (Figure 4). Intensity of the TDS spectra was normalized by the volume of film specimen. Major water-related species desorbed from films were

(24) Irvine, J. T. S.; Sinclair, D. C.; West, A. R. *Adv. Mater.* **1990**, *2*, 132.

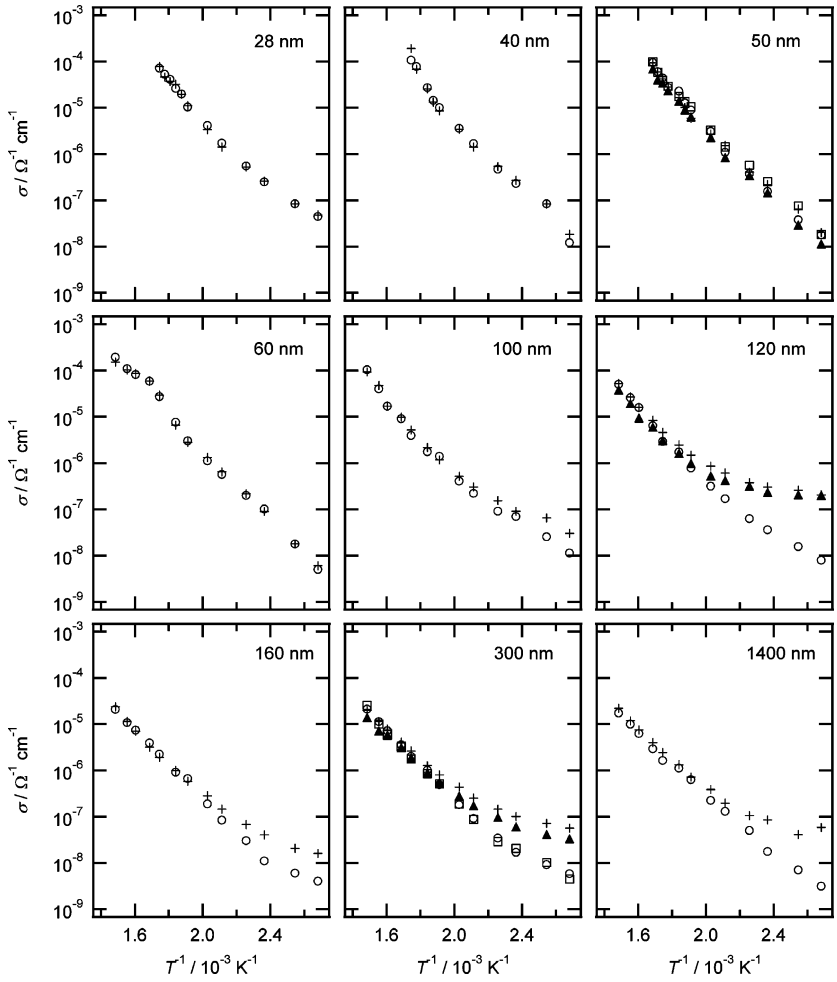

Figure 2. Arrhenius plots of proton conductivity σ of amorphous $Al_{0.1}Si_{0.9}O_x$ thin films with different thicknesses. The conductivity in dry air (○), in H_2O/air (+), in D_2O/air (▲), and in H_2O-saturated 1%-H_2/Ar (□).

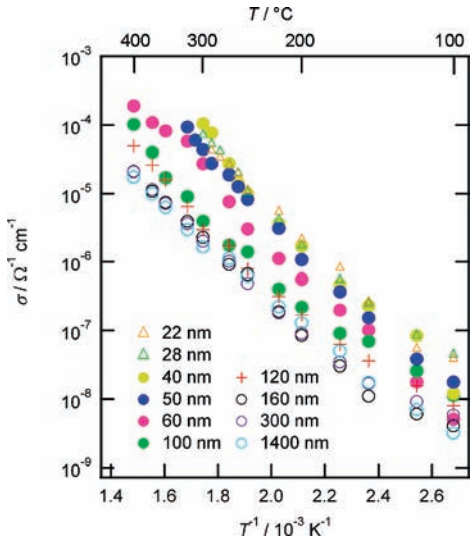

Figure 3. Arrhenius plots of σ of amorphous $Al_{0.1}Si_{0.9}O_x$ film with different thicknesses in dry air.

H_2O (m/z = 18), HDO (m/z = 19) and D_2O (m/z = 20). The amount of desorbed CH_4 (m/z = 16), CO (m/z = 28) and CO_2 (m/z = 44) was very small in the measured temperature range, suggesting that the desorbed water is not a product of combustion of contaminant organic species in $Al_{0.1}Si_{0.9}O_x$ films. In all

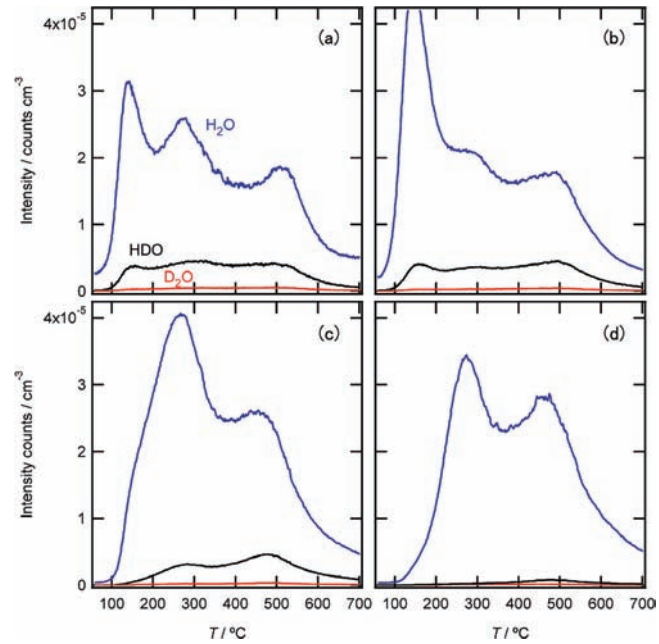

Figure 4. TDS spectra of waters of amorphous $Al_{0.1}Si_{0.9}O_x$ films with thickness of (a) 50, (b) 120, and (c) 300 nm, and (d) 300 nm thick SiO_x film. H_2O (m/z = 18) (blue), (b) HDO (m/z = 19) (black), and D_2O (m/z = 20) (red).

films,the total amount of the desorbed species increases in the order of H_2O > HDO > D_2O, and the amount of D_2O is much lower than those of H_2O and HDO.

The *a*-$Al_{0.1}Si_{0.9}O_x$ films exhibit two or three peaks in the desorption spectra of water (H_2O, HDO and D_2O) at around 150, 280, and 500 °C. The $Al_{0.1}Si_{0.9}O_x$ films of 50 and 120 nm thickness show a strong desorption peak of water at around 150 °C and a middle peak at around 280 °C. The films does not exhibit irreversibility in conductivity during heating and cooling process below 400 °C,[22] so that the desorption at these temperatures does not cause the structural deformation of films. Therefore, the peak at 150 and 280 °C can be assigned to the physically adsorbed water and chemically bound water, respectively. The water desorbed at around 150 °C may not contribute to the elevated conductivity at higher temperatures. On the other hand, a 300 nm thick $Al_{0.1}Si_{0.9}O_x$ film shows the weak shoulder peak of the physically adsorbed water at around 150 °C and shows a very strong peak of the chemically bound water at around 280 °C. Apparently, the H_2O-desorption peak at 280 °C of the 300 nm thick film is much larger than those of the thinner films. This indicates that most of the adsorbed water is chemically bound to the 300 nm-thick film and thus most of them are stable until 280 °C. All the films show the clear peaks of water desorption at around 500 °C, indicating the existence of the proton stable at the temperature. The water present up to this temperature must be related to the elevated conductivity above 300 °C.

The TDS peaks of H_2O and HDO at around 500 °C were fitted with Gaussian function after subtracting the background by linear approximation, and the peak areas are roughly estimated. The peak-area ratio of H_2O/HDO is about 3 in the 50 and 160 nm thick films and about 4 in the 300 nm thick film. It is difficult to determine the mole fraction of D atoms in films from this result, because the background of H_2O due to contaminations is very high. However, it clearly shows that only a part of protons is substituted through the self-diffusion by D_2O treatment. The films apparently show the isotope effect in σ as shown in Figure 2. These results suggest that only a small portion of protons in film is responsible to the proton conductivity of films.

The 300 nm thick SiO_x film exhibits the peaks of water at 270 and 480 °C. The total H_2O-peak area of the SiO_x film is in the same range of that of the 300 nm-thick $Al_{0.1}Si_{0.9}O_x$ film, but the total HDO-peak area of the former is less than 7% of that of the latter. This suggests that the concentration of diffusive protons in a SiO_x film is much smaller than that of $Al_{0.1}Si_{0.9}O_x$ films. This is in agreement with the results that proton conductivity of SiO_x film is 5 orders of magnitude smaller than that of $Al_{0.1}Si_{0.9}O_x$ film.[20,21] It is reported that thermally stable protons in the silica gel film exist as the form of silanol group (Si−OH).[25] Accordingly, it is concluded that most of the silanol groups is not diffusive and the concentration of the protonic carriers of SiO_x film is much smaller than that of $Al_{0.1}Si_{0.9}O_x$ film.

Al K-edge XANES spectroscopy was carried out with $Al_{0.1}Si_{0.9}O_x$ films of 50, 120, and 300 nm thickness (Figure 5). It is reported that Al K-edge spectra are very sensitive to the local environment of Al atoms in oxides.[26,27] Here, the Y-zeolite

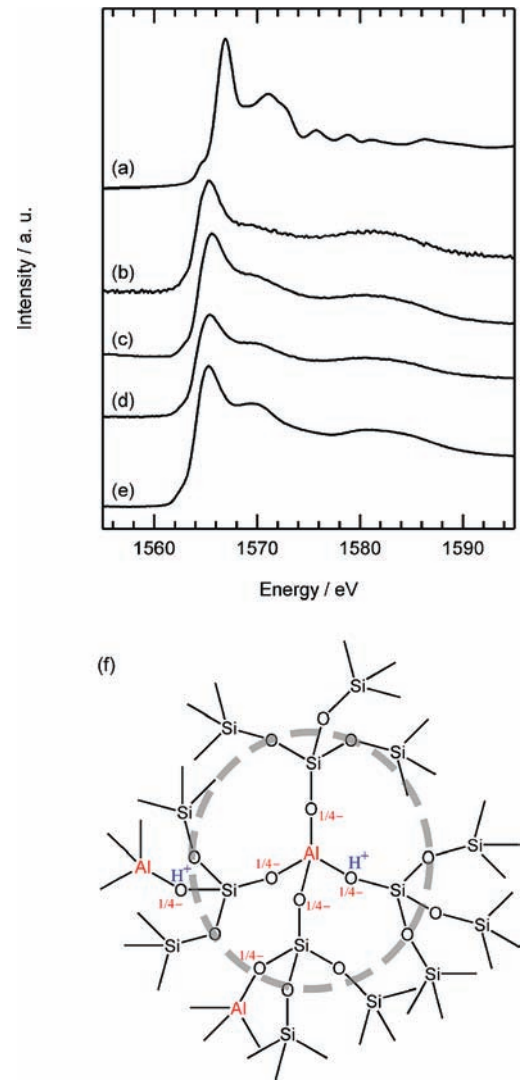

Figure 5. Al K-edge XANES spectra of amorphous $Al_{0.1}Si_{0.9}O_x$ films and reference materials: (a) α-Al_2O_3 powder, (b) 300 nm thick film, (c) 120 nm thick film, (d) 50 nm thick film, and (e) Y-zeolite powder. (f) Schematic representation of the Brønsted acid center of alminosilica tetrahedral network. The dotted circular area shows the unit structure of the acid center.

was used as a reference material of tetrahedral AlO_4 configuration and α-Al_2O_3 as that of octahedral AlO_6 configuration, respectively. Y-zeolite shows a sharp peak at 1566 eV and a broad peak at 1571 eV in agreement with the spectral features of tetrahedral AlO_4 compounds.[26,27] α-Al_2O_3 shows two sharp peaks at 1568 and 1572 eV, which are identical to the features of the compound given by the previous reports.[26,27] The $Al_{0.1}Si_{0.9}O_x$ films possess the same features of XANES in every thickness. They show a sharp peak at 1566 eV and a broad peak at 1571 eV, which are identical to that of Y-zeolite. Accordingly, Al atom in these films preferably takes the tetrahedral AlO_4 configuration. These results suggest that $Al_{0.1}Si_{0.9}O_x$ films have the zeolite-like aluminosilicate network, where the SiO_4 tetrahedron and AlO_4 tetrahedron are 3-dimensionally linked by corner-sharing. Hence, our films can retain amounts of Brønsted acid site by the protonation onto the negative charge of a −Si−O−Al− hetero bond as is the case with zeolite. The schematic representation of Brønsted acid center of amorphous aluminosilicate film is displayed in Figure

(25) Nogami, M.; Abe, Y. *Phys. Rev. B* **1997**, *55*, 12108.
(26) Kato, Y.; Shimizu, K.; Matsushita, N.; Yoshida, T.; Yoshida, H.; Satsuma, A.; Hattori, T. *Phys. Chem. Chem. Phys.* **2001**, *3*, 1925.
(27) van Bokhoven, J. A.; van der Eerden, A. M. J.; Koningsberger, D. C. *J. Am. Chem. Soc.* **2003**, *125*, 7435.

5f. The molecular formula of an acid center is given by $[AlO_4H(SiO)_2]$.

Discussions

The protons related to the elevated proton conductivity of *a*-$Al_{0.1}Si_{0.9}O_x$ films at relatively high temperatures must be involved in the acid sites of aluminosilicate framework. TDS results clearly show that several kinds of protons exist inside the film: One is stable below 300 °C and the other persists until 500 °C. It is reported that amorphous aluminosilicates possess both of Brønsted acid sites and Lewis acid sites.[28−34] These are the active center for various catalytic process,[28,30] and are significantly stable at the catalytic process temperatures above 400 °C.[28,32] Brønsted acid sites are given by the bridging oxygen of Si−O−Al heterobonds as shown in Figure 5f, and Lewis acid sites are basically formed by association of water molecules and oxygen vacancy on Al atoms as follows.[28,33,34]

$$V_O^{\bullet\bullet} + H_2O \rightarrow 2H_i^{\bullet} + O_O^{\times} \quad (1)$$

These suggest that the conductivity based on a Brønsted acidic proton is not dependent on the humidity of atmosphere but the conductivity based on a Lewis acidic proton is humidity-sensitive. The conductivity of a relatively thick film ($d > 120$ nm) drastically changes with humidity at temperatures below 300 °C, but not influenced by humidity at temperatures above 300 °C (Figure 2). Therefore, the conductivity of the thick films below about 300 °C can be related to the protons on Lewis acid site. The increment of σ of the relatively thick film in wet air is due to the increase of Lewis acidic protons (carrier) by reaction 1. The water desorption peak at around 300 °C must be due to the loss of Lewis acid site by the reverse reaction of 1, and thus, the Lewis acidic protons do not affect the conductivity above the temperature. Furthermore, the elevated conductivity above 300 °C of $Al_{0.1}Si_{0.9}O_x$ films can be identical to the migration of native protons on Brønsted acid site, because the conductivity is humidity-insensitive. Therefore, the water desorption at around 500 °C is attributed to the loss of proton on Brønsted acid site. This dehydration follows the loss of the protons and oxide ions composing the framework, so that it must also involve the structural deformation. This is the reason for the dielectric breakdown of films at around 500 °C.

The100 nm-thick films exhibit E_a of σ of 0.5 eV in dry air below 200 °C and 0.2−0.4 eV in wet air below 270 °C, where the conductivity in basis of the Lewis acidic protons is dominant. These E_a values are very similar to those of the perovskite-type $ACeO_3$-[35] or $AZrO_3$-based[36] ceramic proton conductor (A = Ba, Sr) (0.4−0.5 eV). This result is consistent with the fact that the protonic carriers in the ceramic proton conductors are given by the association of water and oxygen vacancy, namely, reaction 1.[3,35] It is clear that the elevated σ at relatively high temperatures ($T > 300$ °C) based on the migration of a native proton on Brønsted acid site accompanies a relatively large E_a (0.7−0.9 eV) in every thickness. Theoretical calculations reported by Sierka et al. indicate that the proton jump barriers between the neighboring Brønsted acid sites in various types of zeolite are in the range of 0.7−1.0 eV.[37] In addition, Hibino et al. reported that the mordenite-type zeolite exhibits the proton conductivity with E_a of about 0.9 eV under dry atmosphere.[12] These values are in agreement with our measured E_a of the conductivity related to Brønsted acid site.

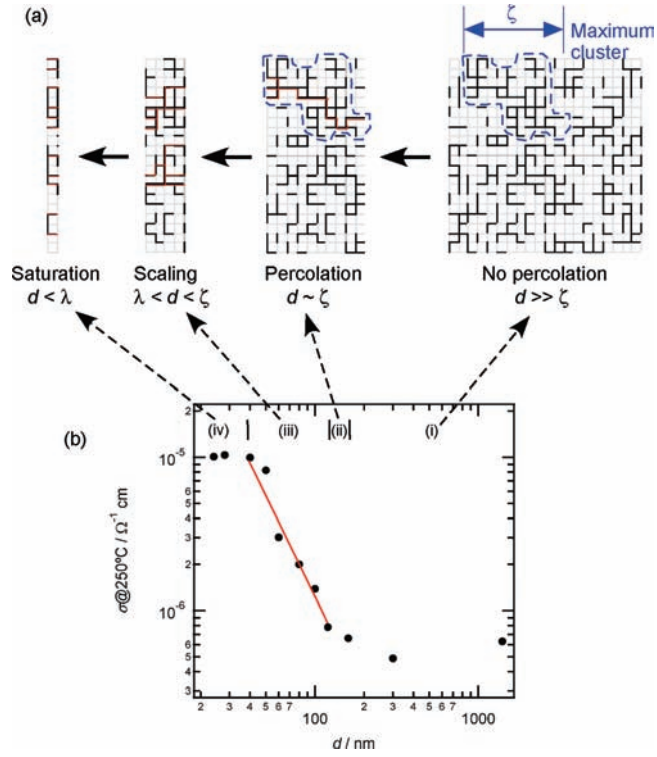

Figure 6. (a) Bond percolation in 20 × 20 square lattice. The calculation is performed with a bond population of 0.35. (b) Log−log plot of σ at 250 °C in dry air vs d.

Apparently, thin films with $d < 100$ nm show the predominant transport of Brønsted acidic protons at any measured temperature. This is curious, as protons given by reaction 1 should diffuse from surface into the film interior more efficiently with thinner films. The σ values below 250 °C of sub-100 nm thick films are lower than those of the films of more than 120 nm-thick in wet atmosphere, indicating that the transport of Lewis acidic protons in the films is lowered in the thickness region of less than 100 nm. The detail mechanism cannot be clarified in this study.

One remarkable feature is the elevated proton conductivity of amorphous $Al_{0.1}Si_{0.9}O_x$ films by reduction of film thickness. Figure 6b shows the log σ−log d plot at 250 °C in dry air. The conductivity under these conditions is based on the Brønsted acidic proton, since the film is once heated at 400 °C in dry air and most of Lewis-acidic protons are lost. The thickness

(28) Tanabe, K.; Misono, M.; Ono, Y.; Hattori, H. *New Solid Acids and Bases*; Elsevier: Amsterdam, 1989.
(29) Crepeau, C.; Montouillout, V.; Vimont, A.; Mariey, L.; Cseri, T.; Mauge, F. *J. Phys. Chem. B* **2006**, *110*, 15172.
(30) Trombetta, M.; Busca, G.; Rossini, S.; Piccoli, V.; Cornaro, U.; Guercio, A.; Catani, R.; Willey, R. J. *J. Catal.* **1998**, *179*, 581.
(31) Hunger, M. *Catal. Rev.* **1997**, *39*, 345.
(32) Bronnimann, C. E.; Chuang, I.-S.; Hawkins, B. L.; Marciel, G. E. *J. Am. Chem. Soc.* **1987**, *109*, 1562.
(33) Chizallet, C.; Rayboud, P. *Angew. Chem., Int. Ed.* **2009**, *48*, 2891.
(34) Omegna, A.; van Bokhoven, J. A.; Prins, R. *J. Phys. Chem B* **2003**, *107*, 8854.
(35) (a) Iwahara, H.; Shimura, T.; Matsumoto, H. *Electrochem.* **2000**, *68*, 154. (b) Kreuer, K. D.; Dippel, T.; Baikov, Y. M.; Maier, J. *Solid State Ionics* **1996**, *86−88*, 613.
(36) (a) Cevera, R. B.; Oyama, Y.; Miyoshi, S.; Kobayashi, K.; Yagi, T.; Yamaguchi, S. *Solid State Ionics* **2008**, *179*, 236. (b) Yajima, T.; Suzuki, H.; Yogo, T.; Iwahara, H. *Solid State Ionics* **1992**, *51*, 101. (c) Sundell, P. G.; Bjorketun, M. E.; Wahnstrom, G. *Phys. Rev. B* **2007**, *76*, 0943011–0943017.
(37) Sierka, M.; Sauer, J. *J. Phys. Chem. B* **2001**, *105*, 1603.

dependency can be divided into four regimes. In regime-i $d >$ 160 nm, the σ is thickness-independent and is at low level. The σ starts increasing in regime-ii at around 120 nm. In regime-iii 40 nm $< d <$ 120 nm, the σ increases in a power low with decreasing film thickness (size-scaling of σ), and in regime-iv $d >$ 40 nm, the σ becomes thickness-independent again and keeps the high value. As a result, σ of the 40 nm thick film is higher than that of the 120 nm thick film by about 30 times. Because these observations bear interesting implications to the physicochemical mechanism of ionic conduction and possible technical applications, we will discuss these aspects in detail.

The power-law scaling of proton conductivity in $Al_nSi_{1-n}O_x$ thin films is characteristic of the percolative conduction system,[38−41] indicating that the $Al_nSi_{1-n}O_x$ nanofilm has a conductive channel penetrating through the poorly conductive matrix. Figure 6a is the two-dimensional representation of the geometrical model for percolation conductivity in $Al_nSi_{1-n}O_x$ film. It shows the bond percolation on a square lattice, where black bond randomly occupies the edge of the lattice with a constant probability P of 0.35 which is less than the percolation threshold P_c (0.5).[38] Here, the glass network of aluminosilicate is approximated by a square lattice, and the black bond represents the conductive path with an average length of λ. It is assumed that proton can effectively migrate through the connection of black bonds and thus the 'cluster' of the connected bonds behaves as a proton conductive channel. In the present case ($P < P_c$), the clusters with various finite lengths are accumulated inside the glass and the number of clusters with the length l increases with decreasing l (finite-size scaling).[38] As a result

$$N(l, \zeta) \propto (l/\zeta)^{-\tau} \quad (2)$$

Here, N is the number of cluster with a length l, and τ is a critical index. Theoretically, the index τ is reported to be 2.3 for the site percolation in a three-dimensional system.[38,42] The solid red line of Figure 6b is obtained by linear fitting for the data in the thickness range of 120−40 nm. The slope is about 2.2 ± 0.2, which is close to the theoretical value of τ.

When the film thickness d is larger than 120 nm, it is longer than ζ, so that conductive clusters become insulated in a poorly conducting matrix and the film remains in the low (normal) conductive phase (regime-i). Scaling of conductivity of our $Al_xSi_{1-x}O_n$ film starts at d of 120 nm, suggesting that ζ in $Al_nSi_{1-n}O_x$ film is in this range. Hence, the conduction path percolates between both electrodes at the thickness (regime-ii). In $d <$ 120 nm (ζ), more conductive clusters percolate with decreasing d (Figure 6a) by following the finite-size scaling (eq 2) and conductivity scaling undergoes (regime-iii). As d decreases more and is in the vicinity of an average length of conductive path λ, the conductivity may be saturated. Accordingly, the thickness-independent conductivity in $d <$ 40 nm is due to the reduction of thickness into the range of λ (regime-iv). This behavior poses one important result that the average length of conductive path in $Al_nSi_{1-n}O_x$ film is in the range of a few tens nanometer.

On the basis of hopping scheme, a proton on one acid site moves to the other empty sites of the neighboring acid center by thermal-activated jump process during conduction. A distance of proton hopping is calculated to be about 0.5 nm, if the acid center is directly connected to the others via vertex sharing. This value is more than 1 order of magnitude smaller than the unit length λ of the conductive path given by conductivity measurements, showing that the site-to-site hopping path is not corresponding to the unit path in the percolative conduction of $Al_{0.1}Si_{0.9}O_x$ film.

Alternative structure for the unit conductive path with the mesoscopically sized dimensions may be the aluminosilicate chain built up by cross-linking of several acid center units. a-$Al_{0.1}Si_{0.9}O_x$ film can be represented as $[AlO_4H(SiO)_2]_{0.3}$-$[SiO_4(SiO)_2]_{0.7}$ by the acid centers $[AlO_4H(SiO)_2]$ and the corresponding inert moiety $[SiO_4H(SiO)_2]$ if the formation of terminal OH group like a silanol is neglected. Such a perfect aluminosilicate framework can be approximated as the distorted diamond lattice. The population of the acid centers, 0.3, is smaller than the percolation threshold P_c of the site percolation in diamond-like lattice (0.43).[38] Therefore, the infinitely sized acid site network does not encounter in a-$Al_{0.1}Si_{0.9}O_x$ film and the growth of the alminosilica network giving high conductive pathway is frequently disturbed by segregation of an inert silica moiety $(-O-Si-O-Si-)_n$. Such a subcritical system must reveal the finite size-scaling behavior in agreement with the results here. TDS results show that the deuterated $Al_{0.1}Si_{0.9}O_x$ film retains a large amount of H atoms that are unexchanged by D_2O treatment, indicating that the film contains abundant silanol group as is the case with SiO_x film. The protons on silanol group is immobile as mentioned above, so that the hopping transport of protons along the acid network must be hindered by the terminal OH groups. Apparently, termination by OH group suppresses the extension of highly conductive pathway so as to lower the conductivity of a thicker a-$Al_{0.1}Si_{0.9}O_x$ film. Accordingly, one possible mechanism for σ scaling is identical to scaling of the length of an aluminosilicate acid network that is segmentalized by OH termination and inert silica segregation.

Conclusions

In summary, it is demonstrated that amorphous $Al_{0.1}Si_{0.9}O_x$ nanofilms were an anhydrous proton conductor at temperatures below 450° due to the thermally stable acid centers on silicate framework. Although the films with thickness d of larger than 100 nm exhibit the humidity-sensitive conductivity related to the Lewis acid sites at relatively low temperatures, the elevated proton conductivity at relatively high temperatures is humidity-independent due to the native protons on Brønsted acid site of the films at any thickness. Furthermore, the $Al_{0.1}Si_{0.9}O_x$ film reveals unique size-scaling behavior of conductivity of the proton on a Brønsted acid site. The proton conductivity in dry air is not dependent on the thickness in $d >$ 120 nm, but it increases in a power low by reduction of thickness in the range of 120−40 nm and it is saturated in $d <$ 40 nm. This conductivity scaling is explicable by the existence of the highly conductive pathway of the zeolitic acid network, which is built by the interconnected Brønsted acid centers. The pure silica moiety does not exhibit strong Brønsted acidity and a proton on terminal OH group is immobile. These components suppress the extension of the highly conductive acid network, and the networks with various lengths from a few tens to hundreds of nanometers accumulate inside the film. This is the origin for the σ scaling in $Al_{0.1}Si_{0.9}O_x$ film.

(38) Stauffer, D.; Aharony, A. *Introduction to Percolation Theory*; CRC Press: New York, 1991.
(39) Berkemeier, F.; Abouzari, M. R. S.; Schmitz, G. *Phys. Rev. B* **2007**, *76*, 0242051.
(40) Vegiri, A.; Varsami, C. E. *J. Chem. Phys.* **2004**, *120*, 7689.
(41) Snow, E. S.; Novak, J. P.; Campbell, P. M.; Park, D. *Appl. Phys. Lett.* **2003**, *82*, 2145.
(42) Jan, N. *Physica A* **1999**, *266*, 72.

Apparently, the superior conductivity of a-$Al_{0.1}Si_{0.9}O_x$ film is related to the development of 3-dimensional network of the interconnected SiO_4 and AlO_4 tetrahedra. Extension of this interconnected network to macroscopic regime is the great challenge in view of tailoring ionic transport properties of solids. The emergence of infinite-sized acid site network may largely enhance the proton conductivity of aluminosilicate material if any thickness. Unfortunately, it is difficult to suppress the formation of terminal hydroxyl group in the films by usual sol−gel film deposition. The Al/Si mole ratio is needed to increase from 1/9 in the present film to 1/6 in order to get above P_c of the site percolation in diamond lattice. The concentration and distribution of Al must be controlled in atomic precision to form the aluminosilicate network with desirable MO_4-tetrahedal arrangement. The process to improve simultaneously the population of Brønsted acid centers and the terminal OH groups will be a key to designing a more efficient ionic conductor.

The percorative scaling behavior reported here is the first example for the proton conduction in solids, but this phenomenon must be common for groups of the ionic conductors revealing structural inhomogeneity. Various amorphous materials and nanocrystalline solids, nanocomposite materials etc., will be adopted into this group. Our findings strongly suggest that these ionic conductors essentially involve the mesoscopically sized ionic channels inside a matrix and have the potential to tune the conductivity by downscaling even though the bulk materials do not reveal high conductivity. Examining the conductivity scaling behavior will be powerful in identifying the length and unit structure of conduction pathway. These topological considerations should be extremely useful for the development of various cationic and anionic conductors based on the nanostructured materials. The current results open up the new way to the tailor-made ionic conductor.

Acknowledgment. Part of this work was supported by the Use-of-UVSOR Faciclity Program (B1A, 2008) of the Institute of Molecular Science. This work was financially supported by the Grant-in-Aid of JSPS for Scientific Research on Young Scientists (B) and by the Global COE Program (Project B01: Catalysis as the Basis for Innovation in Materials Science) from the Ministry of Education, Culture, Sports, Science and Technology, Japan.

JA904627H